Supramolecular architecture of $[AsPh_2Br_2]_2[(Br_3)^-\ldots(Br_2)\ldots(Br_3)^-]$ obtained by bromination of $(AsPh_2)_2S$

Luminita Silaghi-Dumitrescu,[a]* Amr A.A. Attia,[a] Radu Silaghi-Dumitrescu,[a] Alexander J. Blake,[b] D. Bryan Sowerby[b]

[a]*Department of Chemistry, Babes-Bolyai University , 1,Kogalniceanu Str.,400084, Cluj-Napoca, Romania*

[b]*School of Chemistry, University of Nottingham, Nottingham NG7 2RD, U.K.*

*Corresponding author e-mail:lusi@chem.ubbcluj.ro;

Abstract

Bromination of $(AsPh_2)_2S$ leads to cleavage of the sulfide bridge to give $AsPh_2Br$ when 1 mol of bromine is used but with 2 mols the product is the polybromide, $[AsPh_2Br_2]_2[Br_8]$, containing the previously unknown $[AsPh_2Br_2]^+$ cation and a rare $[Br_3]^-\ldots[Br_2]\ldots[Br_3]^-$ ensemble whose short (yet not covalent) $Br_2\ldots Br_3$ contacts have previously supported tentative description as an octabromide Br_8^{2-} anion. X-ray crystallography shows that the compound has a three dimensional supramolecular structure based on cooperativity of weak intermolecular C-H...π, C-H…Br hydrogen bonds and secondary Br…Br interactions in the solid state. The electronic structure and the stability of the $[AsPh_2Br_2]_2[Br_8]$ are rationalized using DFT and HF calculations and molecular orbital considerations.

Keywords: arsenic, bromine, Br_8, arsonium, crystal structure, DFT, supramolecular

1. Introduction

We have been interested for some years in reactions of the arsenic(III) bridged compounds, $(AsPh_2)_2E$ where E = O or S, with both oxidising agents and transition metal compounds. Oxidation with either t-butyl hydroperoxide or sulfur led to the mono-oxidation products, $AsPh_2(E)EAsPh_2$, but the corresponding di-oxidation products were hydrolytically unstable and could not be isolated.[1] Attempts to produce mono- and di-oxidation products, $(AsPh_2X_2)O(AsPh_2)$ and $(AsPh_2X_2)_2O$ from the reaction of $(AsPh_2)_2O$ with halogens were also unsuccessful. Even at temperatures as low as –78°C, the As–O–As linkage was always broken and only monoarsenic species were isolated. With an excess of elemental chlorine the oxidation products were diphenylarsenic(V) trichloride, $AsPh_2Cl_3$, and dihydroxodiphenylarsonium chloride, $[AsPh_2(OH)_2]Cl$.[2] Oxidation of $(AsPh_2)_2O$ with elemental chlorine or with SO_2Cl_2 in a 1:1 molar ratio gave the same dihydroxodiphenylarsonium chloride accompanied by diphenylarsenic(III) chloride $AsPh_2Cl$. With an excess of SO_2Cl_2, diphenylarsenic(V) chloride, $AsPh_2Cl_3$, and dihydroxodiphenylarsonium hydrogensulfate $[AsPh_2(OH)_2]$ $[HOSO_3]$ were the products.[2] Reactions with one mol of bromine gave dihydroxodiphenylarsonium bromide, $[AsPh_2(OH)_2]Br$, and diphenylarsenic(III) bromide, $AsPh_2Br$.[3] With two mols of bromine, the course of the reaction was similar, but here both products were arsenic(V) species $[AsPh_2(OH)_2]Br$, and diphenylarsenic tribromide, $AsPh_2Br_3$.[3] The As-O-As bridge was also broken in the reaction of $(AsPh_2)_2O$ with elemental iodine, when diphenylarsenic(III) iodide,

$AsPh_2I$,[4] and diphenylarsinic acid, $AsPh_2$ (O)OH,[5] were separated from the reaction mixture. Reactions of these bridged arsenic(III) compounds with Group 6 metal carbonyls led to products showing a variety of coordination patterns.[6] These reactions have also been investigated theoretically by our group using semiempirical, *ab initio* and DFT methods.[6-8]

In continuation of this work, we now report results of experiments in which $(AsPh_2)_2S$, is oxidised with elemental bromine.

2. Experimental

All experiments were carried out using standard Schlenk methods and anhydrous freshly distilled solvents (dichloromethane, toluene and acetonitrile). Experiments were carried out at both room temperature and at -78^o to try to define conditions for preservation of the As-S-As bridge. The procedure described below refers to the room temperature experiments in dichloromethane; experiments using other solvents (toluene, acetonitrile) and those at -78^o were similar and the products isolated were also the same. Bis(diphenylarsenic) sulfide was prepared according the literature.[18]

2.1. Reaction of $AsPh_2$-S-$AsPh_2$ with Br_2 in molar ratio 1:1

The solution obtained by dissolving $(AsPh_2)_2S$ (0.49 g, 1.0 mmol) in dichloromethane (10ml) was treated with bromine (0.16 g, 1.0 mmol) with stirring at room temperature. After several minutes a yellow waxy product was formed which was shown to be sulphur. The yellow solution was cannulated and the solvent evaporated slowly in an inert atmosphere to give a yellow oil, identified as $AsPh_2Br$**.** (Found: C, 46.24; H, 3.16. Calc. for $C_{12}H_{10}AsBr$: C, 46.60; H, 3.23 %)

2.2. Reaction of $AsPh_2$-S-$AsPh_2$ with Br_2 in molar ratio 1:2

Bromine (0.48 g, 3.0 mmol) was added slowly by a syringe to a solution of $(AsPh_2)_2S$ (0.735 g, 1.5 mmol) in anhydrous dichloromethane (20 ml). An orange precipitate was formed instantaneously. The supernatant solution was cannulated and the precipitate washed with small amounts of CH_2Cl_2 (m. pt 132^{o}C). (Found: C,: 21.44; H, 1.70. Calc. for $[AsPh_2Br_2]_2[Br_8]$: C, 20.34; H, 1.42 %. Mass spectrum: m/z 308 $[AsPh_2Br]^+$, 229 $[AsPh_2]^+$, 227 $[AsPh_2- 2H]^+$, 154 $[Ph_2]^+$, 152 $[AsPh]^+$). The separated solution was evaporated in a vacuum to give a yellow oil shown to be $AsPh_2Br$. Found: C, 46.44; H, 3.06. Calc. for $AsPh_2Br$: C, 46.60; H, 3.23 %). Crystals of the orange solid suitable X-ray diffraction were obtained by slow evaporation of a solution in dichloromethane.

2.3.Molecular orbital calculations

Geometry optimizations and single point calculations were carried out using the B3LYP DFT functional[9, 10] and the HF method coupled with the Dunning's correlation consistent triple-ζ basis set aug-cc-pVTZ[11] and with Grimme's dispersion correction D3.[12, 13] The nature of the stationary points after optimization were checked by calculations of the harmonic vibrational frequencies to insure that genuine minima were obtained. All calculations were performed using the ORCA 3.03 software package.[14] Molecular orbitals were visualized using the UCSF Chimera package.[15] For selected models, calculations were also performed using the BP86/6-31G*, B3LYP/6311+G* and B3PW91/6311+G* DFT methodologies.[16, 17]

2.4.Structure determination for $[AsPh_2Br_2]_2[Br_8]$

Crystallographic data (cf. CCDC 1563861) are summarised in Table 1, which also includes details of the method of solution and the refinement conditions. Data were corrected for Lorentz and polarisation effects, merged and systematically absent reflections removed; an absorption correction was applied. The structure was solved by direct methods (SHELXS-86) and refined by full matrix least squares (SHELXL-93)[18]; hydrogen atoms were placed at their calculated positions and refined riding on their respective carbon atoms. A standard weighting scheme was applied and a correction was made for extinction.

Table 1. Crystallographic data

Empirical formula	$C_{12}H_{10}AsBr_6$
Formula weight	708.59
Crystal size /mm	0.36 x 0.14 x 0.12
Space group	*C*2/*m*
a /Å	23.144(8),
b /Å	9.290(3),
c /Å	8.423(3)
β / º	90.33(3)
U /Å^3	1811. 0 (11)
Z	8
D_c /Mg/m^3	82.599
μ /mm^{-1}	15.100

F(000)	1300
λ /Å	0.71073
T/K	150(2)
Reflections collected	2863
θ range /°	2.98 - 25.01°
Index ranges	-27<=h<=27, O<=k<=ll, -4<=1<=10
Independent reflections	1689 [R(int) = 0.041]
Observed reflections	1394 [I>2σ(I)]
Absorption correction	Numerical (T_{min} = 0.094, T_{max} = 0.278)
Structure solution	Direct and difference Fourier methods
Data / restraints / parameters	1689/26/101 (least-squares on F^2)
Final R indices [I>2σ(I)]	R_1 = 0.0725, wR_2 = 0.1871
Final R indices (all data)	R_1 = 0.0879, wR_2 = 0.2067
Goodness-of-fit on F^2	1.077
Weighting scheme	$w=1/[\sigma^2(F_o^2) + (0.106P)^2+115.90P]$ where $P=(F_o^2 + F_c^2)/3$
Final difference map /$Å^{-3}$	+2.93 and -2.98

3. Results and Discussion

Treatment of $(AsPh_2)_2S$ with one mol of bromine gave a single product diphenylarsenic(III) bromide, $AsPh_2Br$, but when two mols were added, a yellow precipitate was formed in good yield almost immediately. Elemental analysis pointed to a Br:As:C:H ratio of 6:1:12:10 and the product contained neither sulfur from the starting sulfide nor oxygen from hydrolysis. The reaction was reproducible and the product was stable showing no bromine loss after 6 months. The final formula was established by single crystal X-ray diffraction as $[AsPh_2Br_2]_2[Br_8]$ if, as previously done in references [19-22], the short $[Br_3]^-\ldots[Br_2]\ldots[Br_3]^-$ contacts (below the sum of van der Waals radii) are taken as evidence for a single octabromide species. No compound with this composition nor any compound containing the dibromodiphenylarsonium cation has been reported previously. There are only few previously described examples of putative Br_8^{2-} anions: the diquinuclidinium octabromide,[19] the benzyltriphenylphosphonium octabromide $[(Bz)(Ph)_3P]_2[Br_8]$,[20] $[Cu(dafone)_3]$-$(Br_5)(Br_8)_{0.5}\cdot CH_3CN$, (dafone = 4,5-Diazafluoren-9-one),[21] $[BrC(NMe_2)_2)]_2[Br_8]$.[22]

3.1. Structure of $[Ph_2AsBr_2]_2[Br_8]$

The solid-state three-dimensional supramolecular structure of $[AsPh_2Br_2]_2[Br_8]$ features dibromodiphenylarsonium cations and $[(Br_3)_2(Br_2)]^{2-}$ octabromide dianions as building blocks. Bond lengths and angles are listed in Table 2 and a diagram showing the geometry and atom numbering scheme is given in Figure 1.

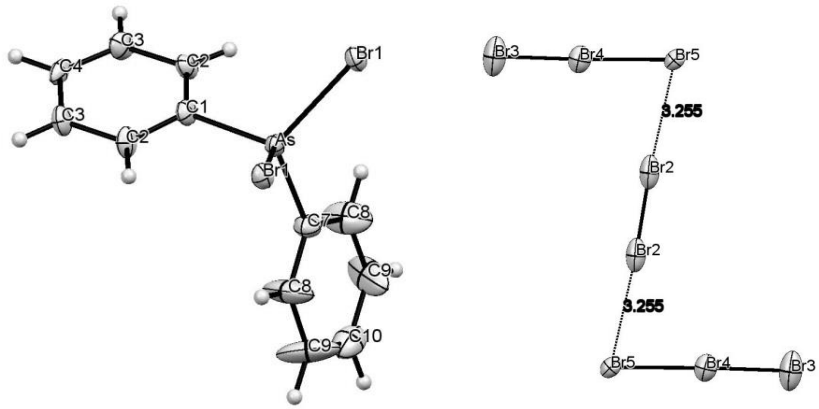

Figure 1. Diagram showing the structure and atom numbering schemes for (a) the $[AsPh_2Br_2]^+$ cation and (b) the $[(Br_3)_2(Br_2)]^{2-}$ / $[Br_8]^{2-}$ anion

Table 2. Selected bond lengths (Å) and angles (°) in $[AsPh_2Br_2]_2[Br_8]$. Primed and double primed atoms are related by the symmetry operations: -x+1,-y+2,-z+1, and x,-y+1,z, respectively

As-Br(1)	2.268(2)
As-C(l)	1.924(16)
As-C(7)	1.911(17)
Br(2)-Br(2')	2.369(6)
Br(3)-Br(4)	2.389(4)
Br(4)-Br(5)	2.672(3)
Br(2)...Br(5')	3.255(4)
Br(1)-As-C(1)	108.9(3)
Br(1)-As-C(7)	107.9(3)
C(1)-As-C(7)	111.9(8)
Br(1)-As-Br(1'')	111. 4 (1)
Br(3)-Br(4)-Br(5)	178.2(2)
Br(4)-Br(5)...Br(2')	76.8(1)

The dibromodiphenylarsonium cation is tetrahedral and lies on a mirror plane with bond angles in the range 107.9 (3)–111.9(8)°. The unique As-Br separation, 2.268(2) Å, is marginally shorter than the equatorial distance in $AsPh_2Br_3$ [2.286(2) Å] and, as expected, substantially shorter than the corresponding axial distance [2.518(2) Å].[2] Axial distances for $AsPh_3Br_2$[23] and As(neo-pentyl)$_3Br_2$[24] are 2.551 and 2.564 Å, respectively. As-Br separations in the isoelectronic As(III) anion $[Ph_2AsBr_2]^-$, as expected, are even longer 2.674(1) Å.[25] As-C bond lengths are normal.

The $[(Br_3)_2(Br_2)]^{2-}$ octabromide dianion, also lying on a mirror plane, is Z-shaped as shown in Figure 1, and can probably best be described as formed from two effectively linear Br_3^- anions interconnected by a Br_2 molecule. Within the anion there are five short Br–Br contacts, i.e. a Br(2)-Br(2') contact of 2.369(6) Å, two Br(3)-Br(4) separations of 2.389(4) Å, and two Br(4)-Br(5) contacts of 2.672(2) Å; in addition there are two longer Br(2)-Br(5) contacts of 3.255(4) Å. These Br-Br contacts are, in fact, very similar to those in the related quinuclidine compound but the Br(4)-Br(5)-Br(2) angles differ widely – 76.8(1)° in the present compound compared with 106.79(4)° in the quinuclidine analogue - probably as a consequence of different crystal packing forces (see later).

There are further weak solid state interactions which link cations and anions in $[AsPh_2Br_2]_2[Br_8]$ to generate a three dimensional supramolecular structure. These can best be understood initially by considering two motifs: firstly dimer formation between two dibromodiphenylarsonium cations and secondly sheet formation from Br_8^{2-}anions.

As shown in Figure 2a, the cations form dimers via short (C)H...π interactions (2.764 Å), which are then further interlinked in pairs (see Figure 2(b)) by two Br(1)....Br(5)...H(C) bridges. Separations here are 3.194 Å [Br(1)...Br(5)] and 2.975 Å [Br(5)-H(C)].

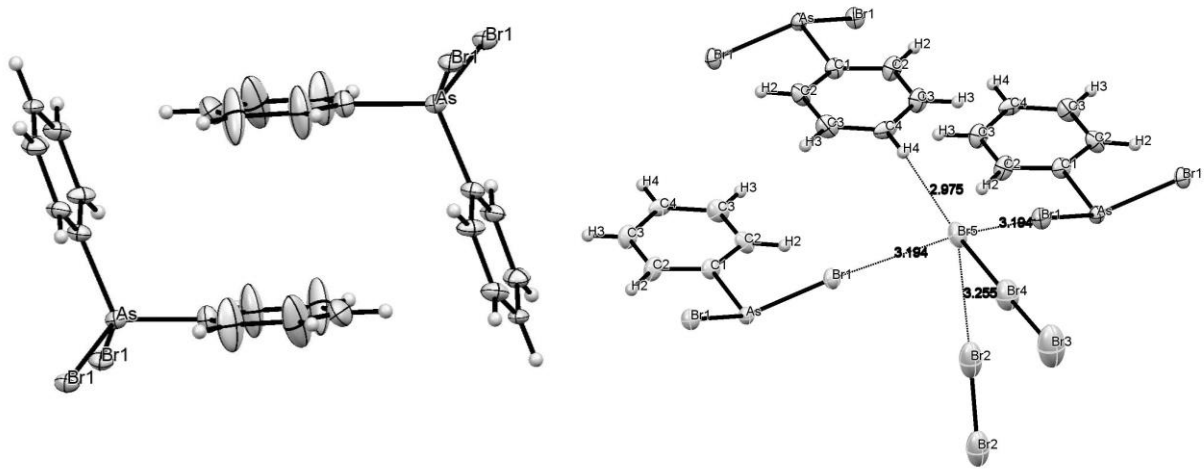

Figure 2. (a) Dimers of the $[AsPh_2Br_2]^+$ cation; (b). further association of two dimers via Br(5) atoms.

The other motif is a sheet (see Figure 3) formed from Br_8^{2-} units associated via Br(2)…Br(3) secondary bonds of 3.381(4) Å. This distance is sensibly higher than the Br(2)…Br(5) separation, 3.225(4) Å, ruling out the possibility of interpreting the structure in terms of Br_{10}^{2-} units.

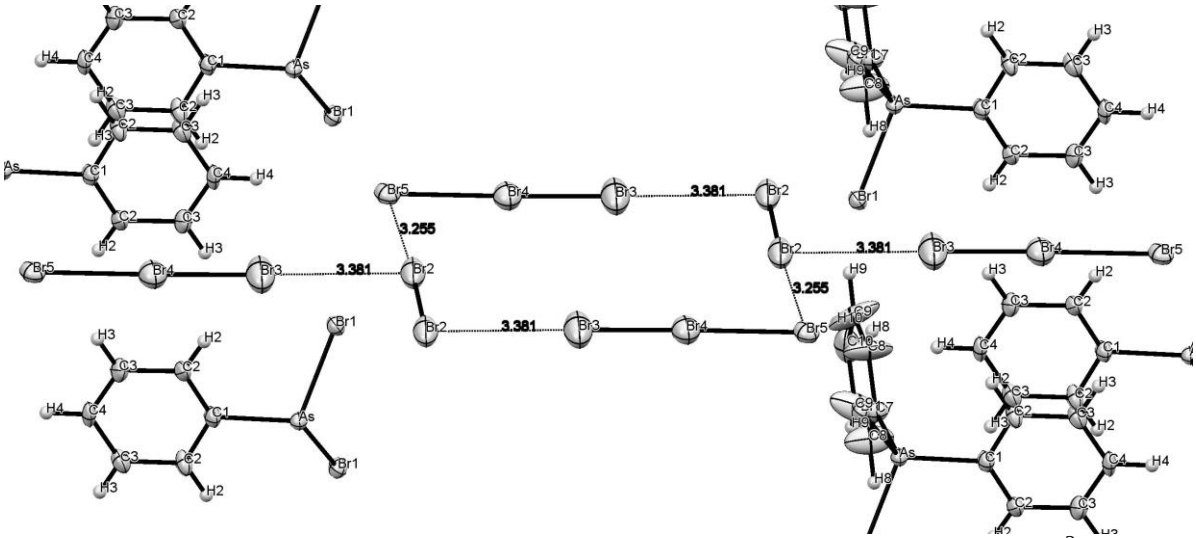

Figure 3. Infinite sheet of bromines formed by association of Z-shaped Br_8^{2-} units.

It is clear at this point that Br(5) is the key to the three dimensional supramolecular crystal structure of the title compound. Each Br(5) atom is in contact with five other bromines (see Figure 2(b)): Br(5)-Br(4) (2.672 Å); Br(5)....Br(2) (3.225 Å) within the Br_8^{2-} unit, two Br(5)...Br(1) and Br(5)...Br(1') (3.194 Å) and a Br(5)...H(C) interaction of 2.672 Å. Angles about Br(5) which direct the packing are: Br(1)-Br(5)-Br(2) 74.64(6), Br(1)-Br(5)-Br(4) 111.41(6), Br(1)-Br(5)-Br(1') 120(x), Br(1)-Br(5)-H(C) 73.4 (y), and Br(4)-Br(5)…H(C) : 170.42(z)°.

The overall structure of the compound shows "channels" containing columns formed by one of the two phenyl groups of the cation (see Figure 4(a)). Two opposite walls of these channels are the bromine sheets described in Figure 3. The other two walls are undulating layers formed by two …Br(5)…Br(1)-As-Br(1)…Br(5)… rows bound together via a (C)-H…Br(5) secondary bond involving the second phenyl group (see Figure 4(b)).

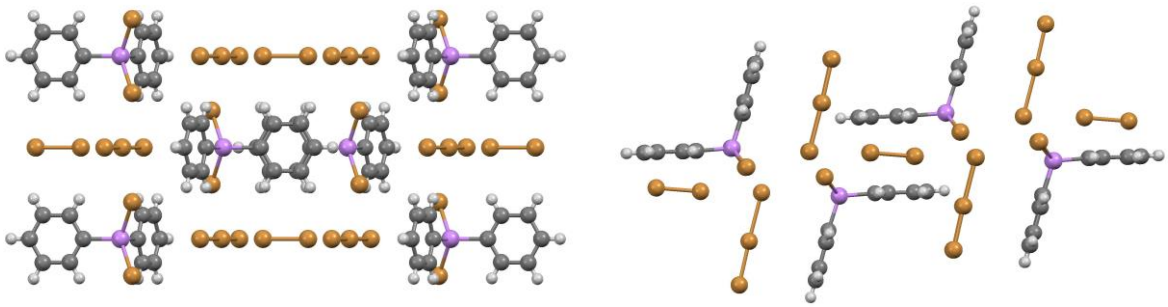

Figure 4. Supramolecular structure, (a) viewed along the c axis, (b) viewed along the b axis.

3.2. Calculated molecular structure of $[(Br_3)_2(Br_2)]^{2-}$ / Br_8^{2-}

Table 3 contains a summary of DFT-calculated Br-Br distances in a Br_8^{2-} anion and, for comparison purposes, there are also experimental values for a number of other (previously assigned/reported) polybromide species. Quinulidine tribromide (QBr_3) was chosen as a Br_3^- example as it contains the same cation as one of the known octabromides. The Br_8^{2-} geometries listed in Table 3 feature a planar *anti* conformation. A *syn* conformation (not shown) was also identified as a local minimum (0.1-0.9 kcal/mol higher in energy compared to *anti*, depending on the density functional employed).

The main structural features of the Br_8^{2-} anion in solid state are retained in isolated ions: i.e. a central Br_2 unit loosely connected to two terminal Br_3^- anions. The more opened gas phase (DFT) structure where the Br(2)-Br(3)-Br(4) angle is 100° is likely due to relaxation on removing the ion from the crystal. The sensitivity of this angle to the nature of the counterion is supported by the values found in solid state for QBr_8 106° [9] and 76.8° in this work. Elongation of the two Br(2)-Br(5) contacts to 3.7 Å (i.e., at the limit of the sum of van der Waals radii), was found to cost 4.6 kcal/mol (B3LYP/ aug-cc-pVTZ) – implying that the strength of a Br_2-Br_3^- interaction is ~2.3 kcal/mol. By the same methodology, the Br(2)-Br(3) contact discussed above cf. Figure 3 (also between a Br_2 and a Br_3^- moiety) was found to b3 0.4 kcal/mol.

Table 3. Experimental and calculated Br-Br contacts in Br_8^{2-} and related polybromide species.

Compound	Bonds in Br_3^- fragments (Å)		Bonds in Br_2 units	Secondary bonds	Br(4)-Br(5)-Br(2) angles
$[AsPh_2Br_2]_2[Br_8]$	2.389(4)	2.672(3)	2.369(6)	3.225	76.80(10)
$2QBr_8$[19]	2.432(1)	2.663(1)	2.354(3)	3.172(1)	106.79(4)

$[(Bz)(Ph)_3P]_2[Br_8]$	251.8	249.8	230.8	310.1	88.0
$[Cu(dafone)_3]$-$(Br_5)(Br_8)_{0.5}\cdot CH_3CN$	2.5213(9)	2.5731(9)	2.3588(12)	3.0374(10)	82.75(3)
$[BrC(NMe_2)_2)]_2[Br_8]$	2.415	2.717		3.018	145.2
Br_8^{2-}, B3LYP/aug-cc-pVTZ	2.560/2.569	2.643/2.647	2.414	3.125	100.5
Br_3^-, B3LYP/aug-cc-pVTZ	2.622	2.622			
Br_2, B3LYP/aug-cc-pVTZ			2.280		
QBr_3[19]	2.457(2)	2.652(2)			
Br_{10}^{2-}[26]	2.91	2.94	2.74 3.50	3.47	
2D Network[27]			2.411(3) 2.357(2)	3.041(3) 3.108(3) 3.197(3)	
Br_2[28]			2.301(1)		

Based on the Br-Br distances, the Br_8^{2-} moiety may be described as a combination of a central Br_2 with two symmetrically placed Br_3^- moieties. For Br_2, it is straightforward to anticipate that the two occupied π^* orbitals and the empty σ^* would participate in bonding with Br_3^-. On the other hand, the Br_3^-frontier orbitals are more complex – and any discussion thereof may benefit from comparison with other triatomics of interest such as I_3^-, N_3^-, O_3 and others. Figure 5 shows the general molecular orbital diagram for a triatomic moiety, drawn as a combination between a central main group element and a pair of two identical atoms; for this latter pair, the contributing orbitals are simple linear combinations (in-phase and out-of-phase) of the respective s and p orbitals. Bonding, antibonding and non-bonding components may be identified in this diagram. For Br_3^-, with a total of 22 electrons, all orbitals except σ^* are occupied. The non-bonding molecular orbitals offer a charge asymmetry, as the central atom is formally not involved in them; this is in line with the partial atomic charges computed for Br_3^- - where the terminal atoms harbor ~0.50 units of charge and the central atom is almost electrically neutral. Similar charge imbalances are computed for other triatomics - F_3^-, Cl_3^-, I_3^-, O_3 and its

congeners S_3 and Se_3, N_3^- and its congeners P_3^- and As_3^-.

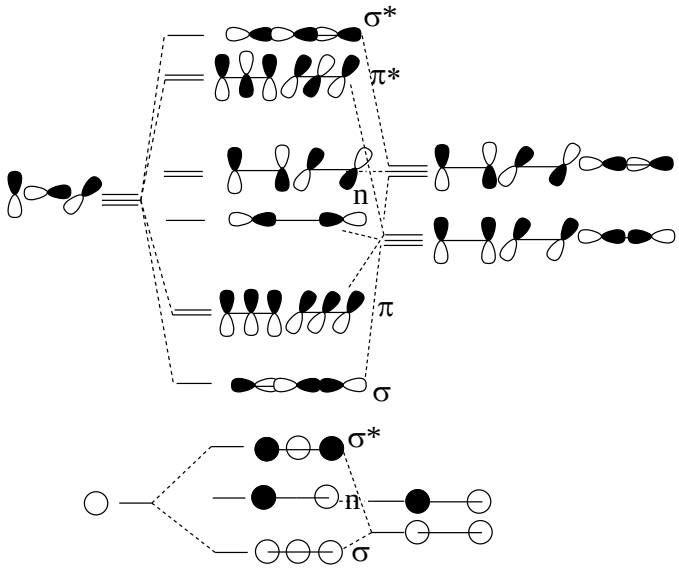

Figure 5. General molecular orbital diagram for a homo-triatomic moiety.

The diagram in Figure 5 would fail to predict the observed linear geometry of N_3^- since the respective 16 electron-configuration would lead to a situation where only one of the two degenerate n(π) orbitals would be occupied – prompting a Jahn-Teller distortion which can only occur via loss of linearity. The diagram would also fail to predict the experimentally-known bent geometry for O_3, since the 18-electron configuration would not lead to a degenerate state and hence would not justify loss of linearity. However, the computed molecular orbitals for N_3^- and O_3 reveal an inversion of relative energies for some of the frontier orbitals: the single n(σ) orbital gains in energy and is now higher than the two π* orbitals; this leaves the O_3 in a degenerate state with respect to the π* orbitals (explaining its non-linearity as a consequence of Jahn-Teller distortion) whereas the N_3^- avoids this situation since its two degenerate HOMO orbitals are both occupied. This inversion of orbital energies seen in O_3 and N_3^- is also observed in S_3, P_3^- and As_3^- but not in Se_3 or in the trihalide anions. Furthermore, the energy separation between the two sets of orbitals may be seen to vary with the covalent radius of the element for group 5 and group 6 elements but not for group 7 elements, as seen in Figure 6. For the group 5 and group 6 triatomics, the holes in the antibonding π orbitals lead to shorter bond lengths so much so that the s orbital of the central atom finds itself in close enough contact with the formally n(σ) molecular orbital to mix and thus raise the energy of the latter. Supporting Information Figure S1 shows graphical representations of the degrees of mixing for several of these species. An extreme illustration of this trend may be seen in the case of Se_3, where the interatomic distance is apparently so large that

mixing of the s orbital becomes sufficiently small to reverse the order of orbitals and to avoid the degeneracy problem – so that Se_3 is, unlike O_3 or S_3, linear; nevertheless, the energy gap remains very low so that one may anticipate that external factors may cause Se_3 to become non-linear. Similar considerations can be made on group 14 triatomic units – where if one equates the C-H bonds with lone pairs then one obtains the allene as isoelectronic with azide with 16 electrons (hence its linearity) while the allyl radical, with one more electron, has partial occupation in the degenerate π* pair of orbitals and is hence bent as a results of a Jahn-Teller distortion. For the halide trianions, there is no net π bonding and all relevant frontier orbitals are occupied, so that there is no possibility of Jahn-Teller distortions. Hence, Br_3^- and its halogen congeners are all linear.

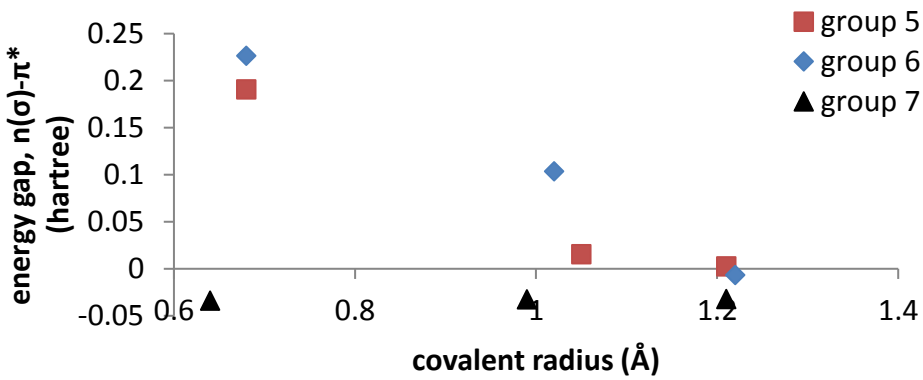

Figure 6. Energy difference between the n(σ) and π* orbitals in F_3^-, Cl_3^-, I_3^-, O_3, S_3, Se_3, N_3^-, P_3^- and As_3^-.

The frontier molecular orbitals of the $[(Br_3)_2(Br_2)]^{2-}$ / Br_8^- moiety, illustrated in Figure 7, reveal simple expected interactions between the set of frontier orbitals of the central Br_2 moiety and the π* and σ* orbitals of the two Br_3^- units. As illustrated in Scheme 1, optimal overlap between these the Br_3^- and the Br_2 orbitals can either occur at 90° or at 180°. Of the Br_3^- and Br_2 frontier orbitals, only the Br_2 σ* and the Br_3^- σ* are empty – and hence only these two orbitals may contribute to net bonding. Indeed, HOMO and HOMO-3 in Figure 7 feature distinguishable Br_2 σ* contributions. This charge donation into Br_2 σ* is reflected in the elongation of the central Br-Br bond relative to an isolated Br_2 molecule by ~0.13 Å (from 2.41to 2.28 Å). However, as LUMO and LUMO+3 feature even stronger Br_2 σ* contributions than HOMO and HOMO-3, one may conclude that the Br_2 σ* remains largely unoccupied (or else, indeed, the Br-Br bond would formally cease to exist). Conversely, as the Br_3^- π* orbitals are transferring part of their electron density to Br_2 via these HOMO and HOMO-3 interactions, one expects that the internal bonds of the Br_3^- moiety would be stronger than in an isolated Br_3^- moiety; however,

here the effects are much smaller than on the Br_2 moiety: indeed: from 2.62 Å in Br_3^-, the Br-Br bonds are shortened on average by 0.3 Å in Br_8^{2-} (to 2.56/2.57 Å for the terminal bonds, 2.64/2.65 for the other ones).

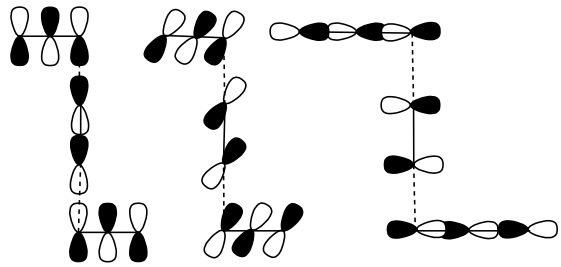

Scheme 1

The partial atomic charges in Table 4 reveal that the Br_3^- and Br_2 moieties are essentially unaffected by complexation to each other : only a total of ~0.1 charge units are transferred to the from the two Br_3^- to Br_2; this is in line with the fact that in Br_8^{2-} the Br_2 σ* orbital (the only one available to receive charge donated by the tribromide anions) has stronger contributions to the LUMO set of orbitals than to the HOMO set of orbitals. Within the Br_3^- moiety, complexation to Br_2 causes a negligible degree of asymmetry/polarization, affecting the partial atomic charges by less than 0.05 units.

While the internal 100° bond angles within Br_8^{2-} are nearly optimal for orbital overlap cf. Scheme 1, distortions of these angles to a range of values seen in the crystal structures appears to only marginally affect the electronic structure. Thus, Table 4 shows that contraction of the angle to 75° or expansion to 140° lead to changes of at most 0.01-0.03 units in the individual partial atomic charges; the energy difference between the computed global minimum and the two hypothetical distorted structures is 2.8 kcal/mol for 75° and 1.5 kcal/mol for 140°. On the other hand, compression of the angle below 75° would entail the central atom of the Br_3 moieties breaching the van der Waals radius of the nearest Br_2 bromine.

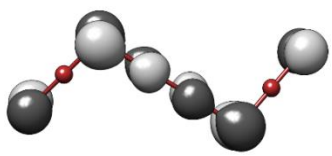

HOMO -10 -7.738

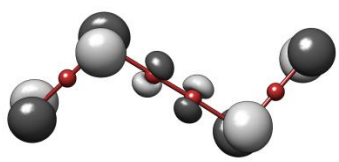

HOMO -9 -7.630

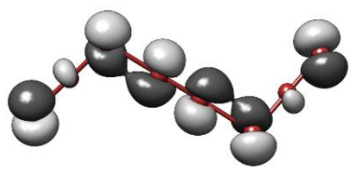

HOMO -8 -7.510

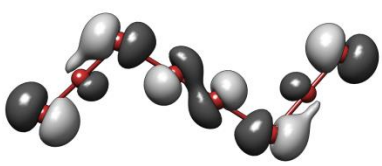

HOMO -7 -7.390

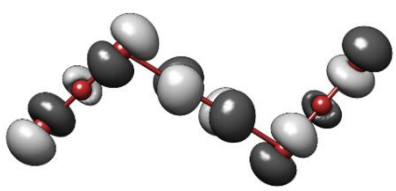

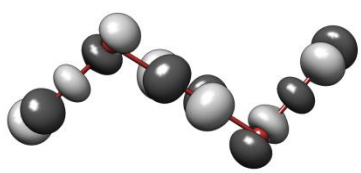

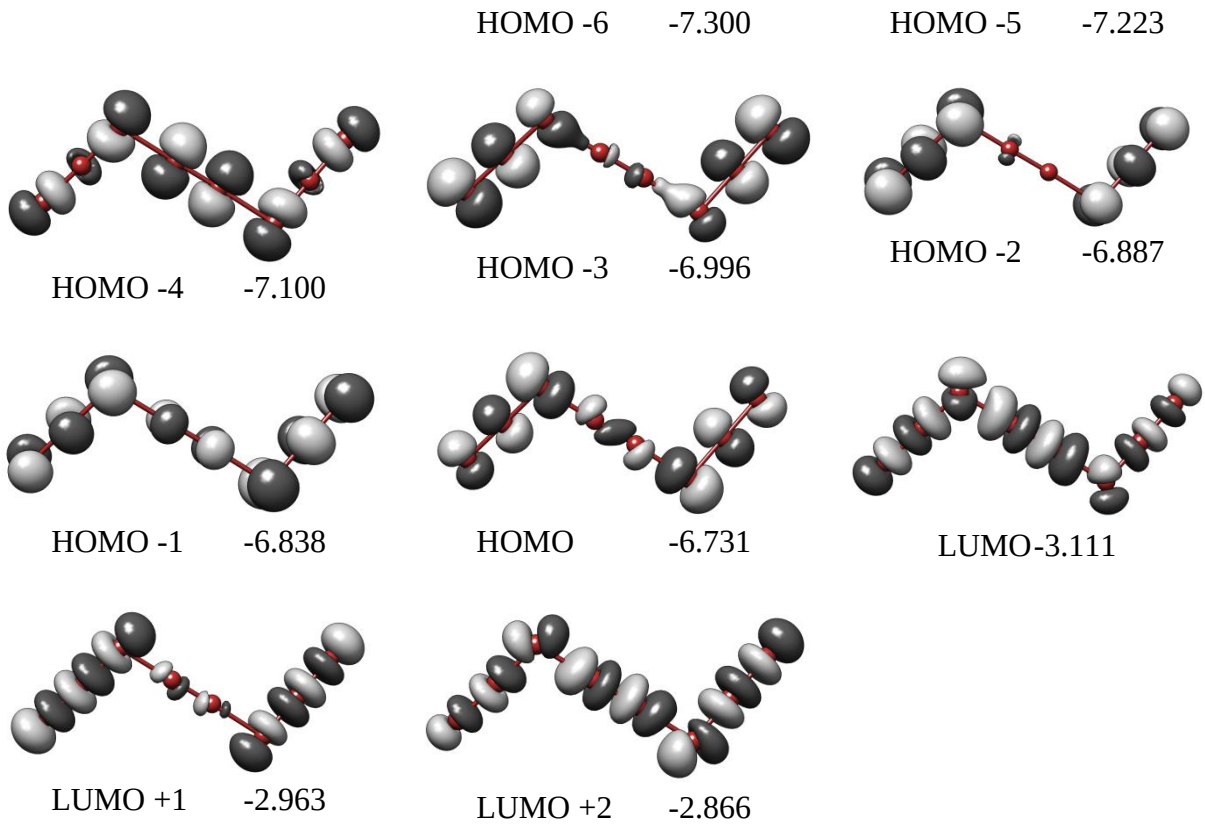

Figure 7. Frontier molecular orbitals for Br_8^{2-} as computed by B3LYP/aug-cc-pVTZ.

Each terminal atom of a Br_3^- moiety in the crystal structure is at less than 4 Å from three surrounding $[AsPh_2Br_2]^+$ units: two identical 3.94-Å distances to a single $[AsPh_2Br_2]^+$ and two single contacts at 3.19 Å with the other two arsonium ions. These latter two distances are ~0.05 Å below the van der Waals radii; however, since Table 4 expectedly shows that the two bromine atoms in this interaction are both negatively charged (e.g., in model $[AsPh_2Br_2]^+[Br_3]^-[Br_2]$), one may conclude that the 3.19-Å contact is due to electrostatic attraction between the arsonium and the Br_8^{2-}, rather than to a discrete Br---Br attractive interaction. The influence of this attractive electrostatic interaction on the Br_3^- is distinctly stronger than the influence of complexation to Br_2, according to the partial atomic charges in Table 4. This is despite the fact that the Br_3^--Br_2 distance is essentially identical to the Br_3^--Br(arsonium) one. Conversely, the arsenic-bound bromine atoms are also measurably affected by the vicinity of the Br_3^- (e.g., in the asymmetric $[AsPh_2Br_2]^+[Br_3]^-[Br_2]$ model the difference in charge between Br and Br* is ~0.1 units).

Table 4. Mulliken atomic charges (HF/aug-cc- pVTZ) for various models: isolated optimized $[Br_8]^{2-}$ and two of its distorted versions (Br-Br-Br angles modified to 75° and 140°, respectively), isolated $[Br_3]^-$, $[AsPh_2Br_2]^+$, $[AsPh_2Br_2]^+[Br_3]^-[Br_2]$ and $[AsPh_2Br_2]^+_6[Br_3]^-_6[Br_2]_4$. For the octabromide, the Br atoms are marked in different shades of grey/black based on which of the three formal components they belong to. For the As-containing models, the atomic coordinates are taken from the crystal structure – with single-point energy calculation.

Atom	Br_8^{2-}	Br_8^{2-} / 140°	Br_8^{2-} / 75°	Br_3^-	$[AsPh_2Br_2]^+$	$[AsPh_2Br_2]^+[Br_3]^-[Br_2]$	$[AsPh_2Br_2]^+_6[Br_3]^-_6[Br_2]_4$
Br1	-0.54	-0.52	-0.57				
Br2	-0.04	-0.05	-0.03			-0.14	-0.12
Br3	-0.04	-0.05	-0.04			0.09	0.07
Br4	0.10	0.09	0.11				
Br5	-0.51	-0.52	-0.51				
Br6	-0.54	-0.52	-0.57	-0.54		-0.29	-0.27
Br7	0.10	0.09	0.11	0.08		0.08	0.07
Br8	-0.51	-0.52	-0.51	-0.54		-0.64	-0.62
As					0.88	0.85	1.05
Br(As)1*					-0.10	-0.03	-0.01
Br(As)2					-0.10	-0.15	-0.08
Ph*					0.16	0.11	0.12
Ph					0.17	0.11	0.12

*differentiated as the As-bound bromine/phenyl closer to the Br_8, in the asymmetric models

Examination of the asymmetric $[AsPh_2Br_2]^+[Br_3]^-[Br_2]$ model also allows one to estimate the effect of the Br_8---phenyl contacts - since in this model only one of the two phenyl moieties is involved in such interactions. However, the total charge per phenyl moiety is essentially unaffected (differences are seen only on the third decimal of partial atomic charges). The larger model, $[AsPh_2Br_2]^+_6[Br_3]^-_6[Br_2]_4$, features partial atomic charges very similar to those of the smaller $[AsPh_2Br_2]^+[Br_3]^-[Br_2]$.

If one describes the potential energy between two dipoles as $-(2\mu_1\mu_2)/(4\pi\epsilon r^3)$, where μ are the respective dipole moments, r is the distance and ϵ is the dielectric constant, a set of two identical dipoles of μ=2, placed at ~7 Å from each other (as is the case for $[AsPh_2Br_2]^+$ in the currently-discussed crystal structure, if one measures the As-As distances), would have an interaction energy of 0.15 kcal/mol. This would then be the stabilization energy added by the dipole-dipole interaction for the antiparallel stacked packing of the As-Ph units in the crystal structure. For each As center, there are also two other distances to take into account, towards two other As at 7.8 Å - which accounts for an additional 0.25 kcal/mol stabilization energy. None of

the short contacts between $[AsPh_2Br_2]^+$ and its neighboring units fall below the limit of van der Waals radii, with the noted exception of a Br-Br contact discussed above as being at most repulsive, and the CH---π interaction also discussed above and for which a value of 1.1 kcal/mol would constitute an upper limit given that in this case the interaction is at the limit of the sum of van der Waals radii[29]). Then, one may interpret that the electrostatic attraction between the counterions, alongside with the dipole-dipole interactions and the CH---π interactions are the driving force for the $[AsPh_2Br_2]^+$ arrangement in the crystal structure.

To conclude, the crystal structure of the polybromide, $[AsPh_2Br_2]_2[Br_8]$ was reported here, containing the previously unknown $[AsPh_2Br_2]^+$ cation and a rare $[(Br_3)_2(Br_2)]^{2-}$ ensemble of a type previously assigned as an octabromide Br_8^{2-}. The crystalline supramolecular structure of $[AsPh_2Br_2]_2[Br_8]$ is based on a complex of weak intermolecular C-H...π, C-H…Br and secondary Br…Br interactions. The electronic structure and the stability of the $[AsPh_2Br_2]_2[Br_8]$ are analysed using DFT and HF calculations, with emphasis on the $[(Br_3)_2(Br_2)]^{2-}$ / Br_8 dianion and on the weak Br_3^-…Br_2 interactions – the nature of which is rationalized both in terms of energies of interactions and in terms of molecular orbitals.

Acknowledgements

We thank the Royal Society (UK), the Romanian Academy and CNCSIS Romania (Grant No. 176C/1999) for financial support.

Supporting Information available: cif data for the crystal structure of $[AsPh_2Br_2]_2[Br_8]$ (as deposited in the Cambridge Crystallographic Data Centre, CCDC 1563861), and plots of frontier molecular orbitals for selected models.

References

[1] L. Silaghi-Dumitrescu, M.N. Gibbons, I. Silaghi-Dumitrescu, J. Zukerman-Schpector, I. Haiduc, D.B. Sowerby, J. Organomet. Chem., 517 (1996) 101-106.
[2] L. Silaghi-Dumitrescu, R. Silaghi-Dumitrescu, A.J. Blake, P.A. Cooke, D.B. Sowerby, Chlorination of (AsPh2)(2)O: Supramolecular structure of dihydroxodiphenylarsonium hydrogensulfate [AsPh2(OH)(2)] [HOSO3], Revue Roumaine De Chimie, 47 (2002) 1063-1068.
[3] L. Silaghi-Dumitrescu, I. Silaghi-Dumitrescu, R. Silaghi-Dumitrescu, I. Haiduc, A.J. Blake, D.B. Sowerby, Bromination of (AsPh2)2O: the structure of tribromo-diphenylarsenic(V). Rev. Soc. Quim. Mexico, 44 (2000) 134-138.

[4] L. Silaghi-Dumitrescu, I. Haiduc, M.N. Gibbons, D.B. Sowerby, Studia Univ. Babes-Bolyai, Ser. Chem., 41 (1996) 43-49.
[5] M. J. Begley, D. B. Sowerby, C. L. Silaghi-Dumitrescu, , , Acta Crystallogr., Sect. C, 51 (1995) 1632-1634.
[6] L. Silaghi-Dumitrescu, S. Pascu, I. Silaghi-Dumitrescu, I. Haiduc, Rev. Roum. Chim., 42 (1997) 747-752.
[7] L. Silaghi-Dumitrescu, R. Silaghi-Dumitrescu, I. Silaghi-Dumitrescu, Studia Univ. Babes-Bolyai, Ser. Chem., 42 (1997) 101-110.
[8] L.H. Doerrer, J.C. Green, M.L.H. Green, I. Haiduc, C.n.N. Jardine, S.I. Pascu, L. Silaghi-Dumitrescu, D.J. Watkin, J. Chem. Soc. Dalton Trans., DOI (2000) 3347-3355.
[9] A.D. Becke, J. Chem. Phys. , 98 (1993) 5648-5652.
[10] C. Lee, W. Yang, R.G. Parr, Development of the Colle-Salvetti correlation-energy formula into a functional of the electron density, Phys. Rev. B, 37 (1988) 785-789.
[11] A.K. Wilson, D.E. Woon, K.A. Peterson, T.H. Dunning, J. Chem. Phys., 110 (1999) 7667-7676.
[12] S. Grimme, J. Antony, S. Ehrlich, H. Krieg, J. Chem. Phys., 132 (2010) 154104.
[13] S. Grimme, S. Ehrlich, L. Goerigk, J. Comput. Chem., 32 (2011) 1456-1465.
[14] F. Neese, The ORCA program system., Wiley Interdisciplinary Reviews - Computational Molecular Science 2(2012) 73−78.
[15] E.G. Pettersen, T.D. Goddard, C.C. Huang, G.S. Couch, D.M. Greenblatt, E.C. Meng, T.E. Ferrin, UCSF Chimera - A Visualization System for Exploratory Research and Analysis, J Comput Chem, 25 (2004) 1605-1612.
[16] S. Spartan, Spartan 5.0, Wavefunction, Inc., 18401 Von Karman Avenue Suite 370, Irvine, CA 92612 U.S.A., Spartan 5.0, Wavefunction, Inc., 18401 Von Karman Avenue Suite 370, Irvine, CA 92612 U.S.A., DOI.
[17] M.J. Frisch, G.W. Trucks, H.B. Schlegel, G.E. Scuseria, M.A. Robb, J.R. Cheeseman, J. Montgomery, J. A., T. Vreven, K.N. Kudin, J.C. Burant, J.M. Millam, S.S. Iyengar, J. Tomasi, V. Barone, B. Mennucci, M. Cossi, G. Scalmani, N. Rega, G.A. Petersson, H. Nakatsuji, M. Hada, M. Ehara, K. Toyota, R. Fukuda, J. Hasegawa, M. Ishida, T. Nakajima, Y. Honda, O. Kitao, H. Nakai, M. Klene, X. Li, J.E. Knox, H.P. Hratchian, J.B. Cross, V. Bakken, C. Adamo, J. Jaramillo, R. Gomperts, R.E. Stratmann, O. Yazyev, A.J. Austin, R. Cammi, C. Pomelli, J.W. Ochterski, P.Y. Ayala, K. Morokuma, G.A. Voth, P. Salvador, J.J. Dannenberg, V.G. Zakrzewski, S. Dapprich, A.D. Daniels, M.C. Strain, O. Farkas, D.K. Malick, A.D. Rabuck, K. Raghavachari, J.B. Foresman, J.V. Ortiz, Q. Cui, A.G. Baboul, S. Clifford, J. Cioslowski, B.B. Stefanov, G. Liu, A. Liashenko, P. Piskorz, I. Komaromi, R.L. Martin, D.J. Fox, T. Keith, M.A. Al-Laham, C.Y. Peng, A. Nanayakkara, M. Challacombe, P.M.W. Gill, B. Johnson, W. Chen, M.W. Wong, C. Gonzalez, J.A. Pople, Gaussian 03, Revision C.02, ; Gaussian, Inc., Wallingford CT, 2004, Gaussian 03, Revision C.02, Frisch, M. J.; Trucks, G. W.; Schlegel, H. B.; Scuseria, G. E.; Robb, M. A.; Cheeseman, J. R.; Montgomery, Jr., J. A.; Vreven, T.; Kudin, K. N.; Burant, J. C.; Millam, J. M.; Iyengar, S. S.; Tomasi, J.; Barone, V.; Mennucci, B.; Cossi, M.; Scalmani, G.; Rega, N.; Petersson, G. A.; Nakatsuji, H.; Hada, M.; Ehara, M.; Toyota, K.; Fukuda, R.; Hasegawa, J.; Ishida, M.; Nakajima, T.; Honda, Y.; Kitao, O.; Nakai, H.; Klene, M.; Li, X.; Knox, J. E.; Hratchian, H. P.; Cross, J. B.; Bakken, V.; Adamo, C.; Jaramillo, J.; Gomperts, R.; Stratmann, R. E.; Yazyev, O.; Austin, A. J.; Cammi, R.; Pomelli, C.; Ochterski, J. W.; Ayala, P. Y.; Morokuma, K.; Voth, G. A.; Salvador, P.; Dannenberg, J. J.; Zakrzewski, V. G.; Dapprich, S.; Daniels, A. D.; Strain, M. C.; Farkas, O.; Malick, D. K.; Rabuck, A. D.; Raghavachari, K.; Foresman, J. B.; Ortiz, J. V.; Cui, Q.; Baboul, A. G.; Clifford, S.; Cioslowski, J.; Stefanov, B. B.; Liu, G.; Liashenko, A.; Piskorz, P.; Komaromi, I.; Martin, R. L.; Fox, D. J.; Keith, T.; Al-Laham, M. A.; Peng, C. Y.; Nanayakkara, A.; Challacombe, M.; Gill, P. M. W.; Johnson, B.; Chen, W.; Wong, M. W.;

Gonzalez, C.; and Pople, J. A.; Gaussian, Inc., Wallingford CT, 2004, DOI (2003).
[18] G.M. Sheldrick, SHELXL-93, Institut für Anorganische Chemie der Univerität Göttingen, Germany, 1993.
[19] K.N. Robertson, P.K. Bakshi, T.S. Cameron, O. Knop, Z . Anorg. Allgem. Chem., 623 (1997) 104-114.
[20] M. Wolff, A. Okrut, C. Feldmann, Inorg. Chem., 50 (2011) 11683-11694.
[21] R. Babu, G. Bhargavi, M.V. Rajasekharan, Eur. J. Inorg. Chem., DOI (2015) 4689-4698.
[22] K. Sonnenberg, P. Pröhm, S. Steinhauer, A. Wiesner, C. Müller, S. Riedel, Z. Anorg. Allg. Chem. , 643 (2017) 101-105.
[23] N. Bricklebank, S.M. Godfrey, C.A. McAuliffe, R.J. Pritchard, J.-M. Moreno, J. Chem. Soc., Dalton Trans., DOI (1995) 3873-3879.
[24] J.C. Pazik, C. George, Organometallics, 8 (1989) 482-487.
[25] S. Grewe, T. Haeusler, M. Mannel, B. Rossenbeck, W.S. Sheldrick, Z. Anorg. Allg.Chem., 624 (1998) 613-619.
[26] C.W. Cunningham, G.R. Burns, V. McKee, Inorg. Chim. Acta, 167 (1990) 135-137.
[27] M.C. Aragoni, M. Arca, F.A. Devillanova, F. Isaia, V. Lippolis, A. Mancini, L. Pala, A.M.Z. Slawin, J.D. Woollins, Chem. Commun., DOI (2003) 2226-2227.
[28] B.M. Powell, K.M. Heal, B.H. Torrie, Molecular Physics, 53 (1984) 929-939.
[29] K. Shibasaki, A. Fujii, N. Mikami, S. Tsuzuki, Magnitude of the CH/pi interaction in the gas phase: experimental and theoretical determination of the accurate interaction energy in benzene-methane, J. Phys. Chem. A, 110 (2006) 4397-4404.